Journal of Applied Hydrography

HYDROGRAPHISCHE NACHRICHTEN 11/2024 HN 129

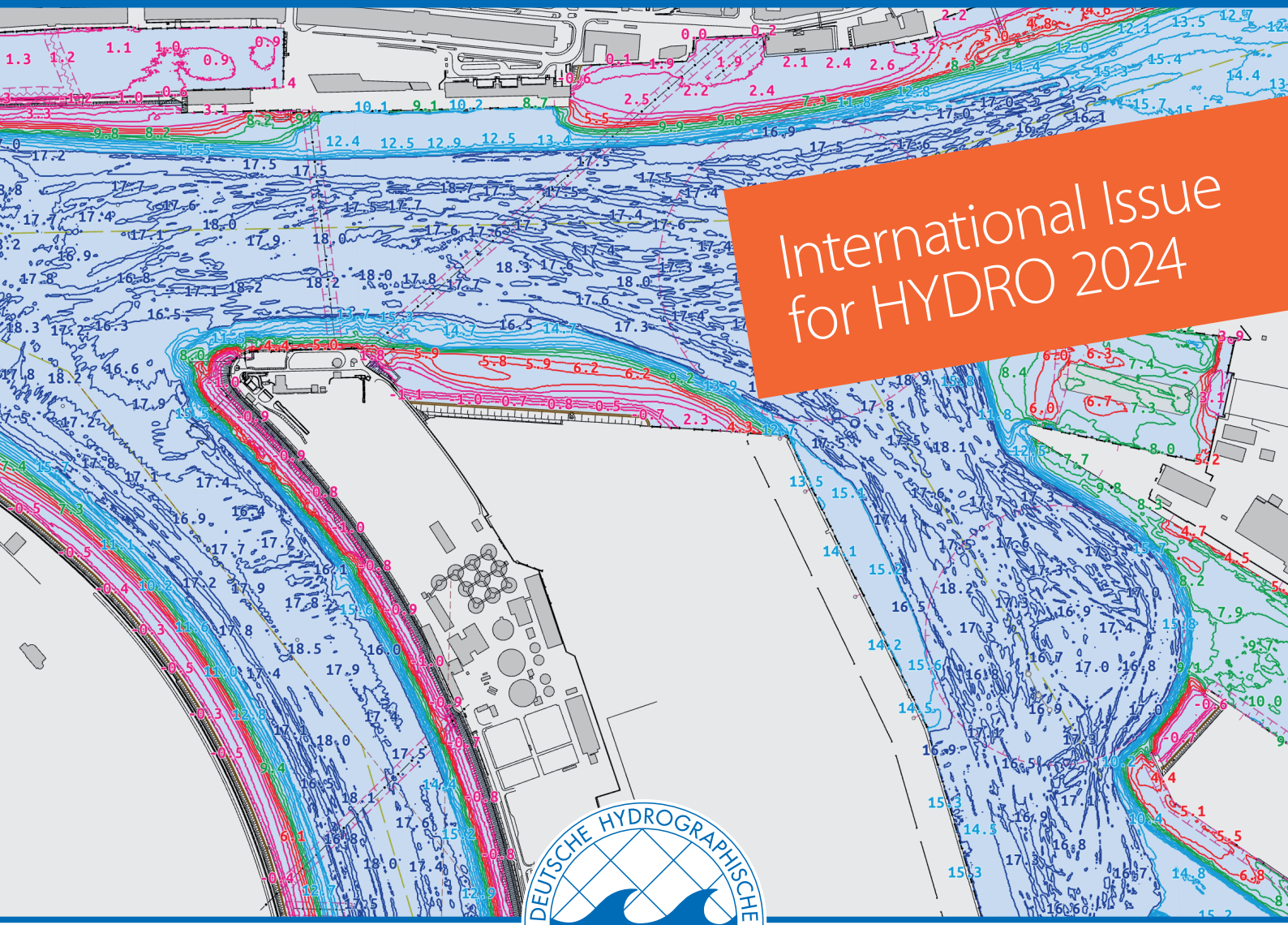

International Issue for HYDRO 2024

DEUTSCHE HYDROGRAPHISCHE GESELLSCHAFT e.V. DHyG

 DOI: 10.23784/HN129-06

Lab experiment for photo bathymetry

Simultaneous reconstruction of water surface and bottom with a synchronised camera rig

An article by LAURE-ANNE GUEGUEN and GOTTFRIED MANDLBURGER

In photo bathymetry, the refraction of the optical rays at the air-water interface, according to Snell's law, causes image blurring and topographic reconstruction errors. Modelling the dynamic, wave-induced water surface can correct this refraction, enhancing bathymetric accuracy. This study presents a technical approach for simultaneously capturing and reconstructing both the water surface and bottom using a synchronised camera rig. Various acquisition configurations were tested to assess the possibility to extract water surface information. The design, acquisition plan, insights and initial results of this feasibility study are discussed, along with suggestions for future improvements and outlooks.

photo bathymetry | water surface | synchronised camera rig | refraction | structure-from-motion
Fotobathymetrie | Wasseroberfläche | synchronisiertes Kamera-Rig | Refraktion | Struktur-aus-Bewegung

Bei der Fotobathymetrie führt die Brechung der optischen Strahlen an der Luft-Wasser-Grenzfläche nach dem Snelliusschen Gesetz zu Bildunschärfen und Fehlern bei der topografischen Rekonstruktion. Die Modellierung der dynamischen, welleninduzierten Wasseroberfläche kann diese Brechung korrigieren und die bathymetrische Genauigkeit verbessern. In dieser Studie wird ein technischer Ansatz zur gleichzeitigen Erfassung und Rekonstruktion der Wasseroberfläche und des Bodens mit Hilfe eines synchronisierten Kamera-Rigs vorgestellt. Es wurden verschiedene Aufnahmekonfigurationen getestet, um die Möglichkeiten zur Gewinnung von Informationen über die Wasseroberfläche zu bewerten. Das Design, der Erfassungsplan, die Erkenntnisse und die ersten Ergebnisse dieser Machbarkeitsstudie werden zusammen mit Vorschlägen für zukünftige Verbesserungen und Ausblicke diskutiert.

Authors
Laure-Anne Gueguen and Prof. Dr. Gottfried Mandlburger conduct research at the Vienna University of Technology, Austria.

laure-anne.gueguen@geo.tuwien.ac.at

1 Introduction

Photo bathymetry is the use of photogrammetry for underwater topography reconstruction. It provides an alternative to traditional acoustic systems which can be more practical and affordable, particularly for water bodies with limited depth and low turbidity like inland rivers or coastal areas. In aerial photo bathymetry, where the imaging systems are above the water, the optical rays must pass through air and water. This is then a case of two-media photogrammetry, requiring the application of Snell's law to correct the refraction of the rays at the interface. As of today, this issue is the main obstacle to achieving high accuracy photo bathymetry.

A 3D model of the water surface is therefore a prerequisite to correct the ray paths, but many current methods simplify the problem by approximating the surface as a static plane, ignoring its dynamic, wave-induced nature. Okamoto (1982) has highlighted that waves introduce substantial errors in underwater topography reconstruction. Existing methods for reconstructing wave patterns are diverse, including the use of surface markers (Chandler et al. 2008) or using the optical properties like specular reflection (Rupnik et al. 2015) or refraction (Murase 1992; Morris and Kutulakos 2011). However, these methods often rely on restrictive assumptions, like previous knowledge of the mean water height or the topography, and are not ideal for reconstructing both the water surface and underwater topography in natural environments.

Our work aims to address these limitations by developing a method for the simultaneous reconstruction of the water surface and bottom, which would then contribute to the development of a solution that would be deployable over inland rivers and coastal areas.

The following sections discuss our methodology, results and future research directions.

2 Methodology

2.1 Goal and design of the experiment

We designed and implemented a lab experiment allowing different data acquisition set-ups for simultaneous capture of the water surface and the

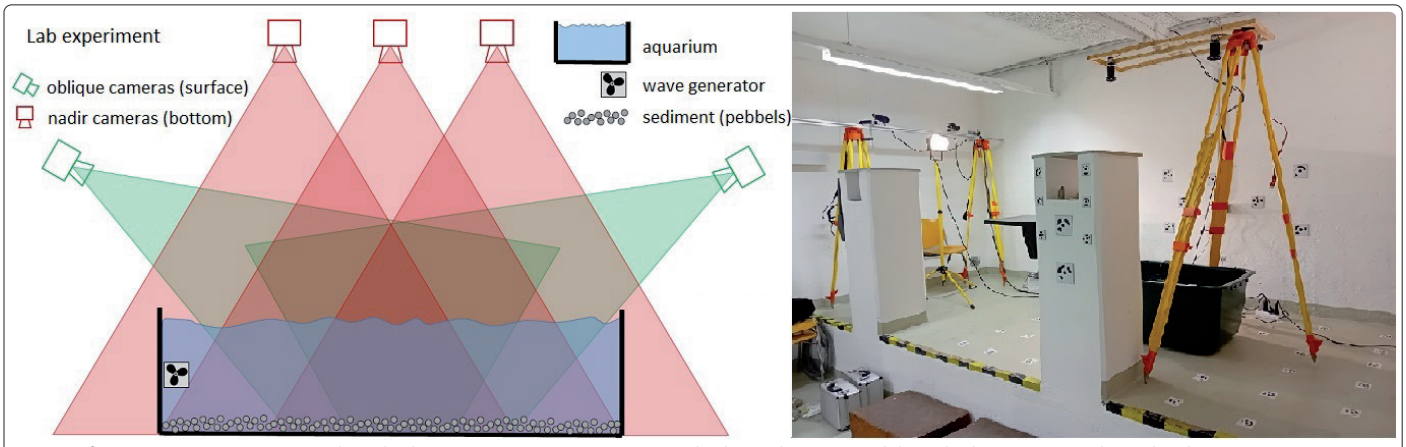

Fig. 1: Left: Data acquisition set-up with multiple static cameras over a water tank. The nadir cameras deliver the bottom via multimedia photogrammetry whereas the oblique cameras are only used for water surface reconstruction. Right: Implementation of the experiment in the measurement lab at TU Wien

water bottom, as illustrated in Fig. 1. The focus of the experiment is to assess the feasibility of (i) capturing and (ii) reconstructing the water surface, which are two distinct issues. Capturing the water surface involves identifying the optimal configuration in terms of equipment, imaging parameters, lighting, positioning, etc. On the other hand, reconstructing the water surface relates to what extent the water surface can be modelled, specifically which parameters can be extracted, which area can be covered, etc. Additionally, this setup is intended as a preliminary step towards a more ambitious experiment, namely surveying inland waters using cameras mounted on a squad of unmanned aerial vehicles (UAVs).

To implement this experiment in the measurement lab of TU Wien, we used a complete camera rig provided by IfP Stuttgart. The setup includes four cameras with lenses, an Arduino Leonardo and the associated cabling. The Arduino functions as a controller, synchronising the cameras by sending an electrical trigger signal at user-defined intervals via a USB connection. Due to technical limitations, the maximum achievable frame rate is 1 Hz, which is the rate used for all results presented in this paper. Two cameras are positioned obliquely from the side to capture the water surface, while the other two are positioned directly above to capture the water bottom. We filled an aquarium with water and added a layer of stones and photogrammetric targets (fixed in a concrete frame) to create a textured topography and to provide checkpoints for later assessment. In addition, we used an indoor fountain pump to generate a dynamic water surface with a regular wave pattern. Setup and equipment are depicted in Fig. 1.

2.2 Preliminary steps

Calibration and geo-referencing

Before conducting the lab experiment, attention was given to calibration and geo-referencing. We use Agisoft Metashape (Over et al. 2021) to estimate the radial distortion, as well as the interior and exterior orientations of the cameras via bundle-block adjustment.

For geo-referencing in the laboratory local coordinate system, we use ground control points (GCP). Approximately 80 coded markers were installed around the scene and surveyed with submillimetre precision using a total station (Leica TS16). These markers were selected to allow automatic detection in Metashape and were strategically placed around the aquarium to function as GCPs and checkpoints. Their placement was carefully considered to align with the cameras' field of view, aiming for an even distribution along the three axes despite the restrictive environment. The markers were measured using angle and distance measurements from six different positions but only angle measurements were used during processing. The coordinates of the points within the laboratory local coordinate system were thus estimated via forward intersection, resulting in a maximum standard deviation of 0.2 mm for any point coordinate.

Reference model

Before filling the aquarium with water and acquiring the data, several images of the aquarium were captured still in dry state using a 28 mm focal length Nikon camera. These images were used to create a reference model of the topography. The final model was generated by applying dense image matching in Metashape and serves as validation. It is presented in Fig. 2.

Acquisition plan

In order to gather a comprehensive dataset and analyse the impact of various parameters, an extensive acquisition plan was implemented in several stages, with each stage building on and improving the previous one based on the insights gained.

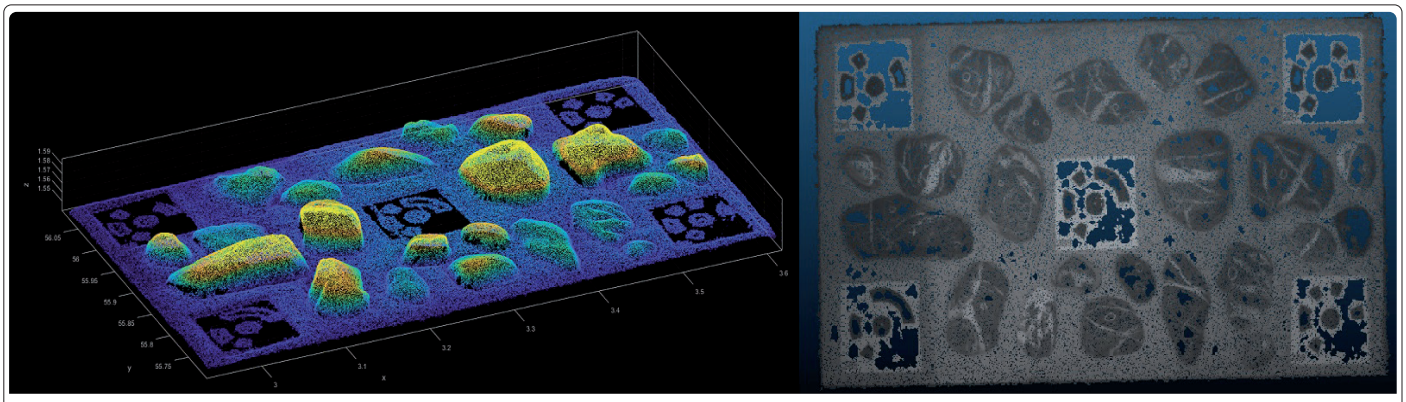

Fig. 2: Reference model of the topography

Two obliquely looking cameras are positioned on the side and two nadir looking cameras above the water tank. The oblique cameras were mounted on a horizontal bar supported by two tripods. The goal of this configuration was to identify tie points on the water surface using a standard Structure-from-Motion approach (Schönberger et al. 2016). Another approach could involve using the specular reflections to derive the surface normal vectors.

For this standard setup, different scenarios were carried out to define the setup that would optimise the number of tie points found on the water surface. In individual scenarios, we tested different heights for the oblique cameras, different levels of turbidity in the water, different lighting setups (position, intensity and subsequent specular reflection) and different camera parameters such as exposure time (3 to 9 ms, depending on the lighting), gamma value (1 or 1.6), gain (0 to 10 %) and aperture (F/1.8 or F/2).

For all scenarios, datasets of 60 frames (equivalent to 1 minute) were collected with a dynamic water surface generated by the pump, and datasets of 20 frames were collected with a flat water surface.

3 Results

3.1 Processing workflow

Our work was primarily focused on the oblique pairs to gain information of the water surface. All acquired data were put through the same processing workflow in Metashape composed of the following steps: feature detection on each image and then matching across the pair, alignment of cameras, geo-referencing with GCPs and dense matching.

The initial results of the processing pipeline applied to all pairs of oblique images showed first and foremost that the perfect transparency of water was a problem because this leads to the tie points being on the topography instead of the water surface. We also observed that most of the tie points on the water surface were located on the specular reflection, meaning that higher specular reflection significantly increases the number of surface tie points. During the iteration of acquisition configurations, we have then decided to add turbidity in the water to get rid of the transparency. And, even though we are aware that an error is induced when a tie point is found on both images where there is specular reflection (due to lighting direction, camera exterior orientations and the

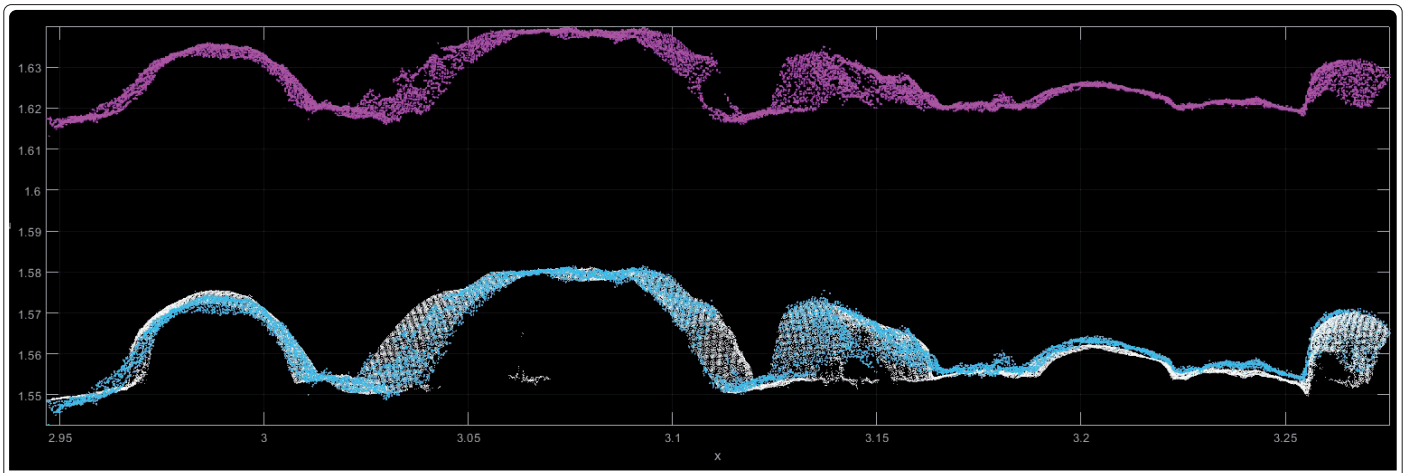

Fig. 3: Profile in XZ plane of the ground truth (white), the model resulting from the four nadir images (magenta) and the model after refraction correction (light blue)

shape of the water surface), we have also decided to maximise the specular reflection to try to obtain more tie points on the water surface.

With enough turbidity to create full opacity in the water column and specular reflection on the surface, the number of tie points on the water surface jumped on average from around two to 50 tie points for a similar pair of images.

3.2 Estimation of mean water height

Using a configuration providing a significant amount of tie points on the water surface, we are able to retrieve the Z coordinate of these tie points, and the average value is therefore an estimation of the mean water height.

To assess this value, we use a model of the topography resulting from four nadir images taken through a flat water surface and we use the Snellius module of the OPALS software (Orientation and Processing of Airborne Laser Scanning data) developed at TU Wien (Mandlburger 2016). The Snellius module allows correcting the refraction effect if the refractive index of water and a 3D model of the water surface are given as input parameters. In our case, we use 1.33575 for the refractive index and the surface is approximated as a flat water surface of height 1.8075 m as this is the parameter to be assessed. The choice of this specific value for the refractive index is detailed in section 3.3.

Fig. 3 shows a profile in the XZ plane of the ground truth and the models of the topography before and after refraction correction. To compare the models with the ground truth, we generate the subsequent digital elevation models (DEM) and compute the histograms of the differences with the DEM of the ground truth.

The results in Table 1 highlight that we are now able to reconstruct the bottom topography with sub-millimetre accuracy compared to the reference model (dry state). This shows that the used technique provides a decent estimation of the mean water height, despite the dynamic nature of the water surface.

3.3 Refractive index of water

During the processing workflow presented in section 3.2, the refraction correction step has been carried out with various values for the refractive index as we had no direct measurement in the context of our lab experiment. We have tested the following values: 1.33, 1.335 and 1.34, but also different mean water heights around the average value of the tie points. The results are presented in Table 2.

The results highlight the significant impact of the refractive index in comparison with the mean water height. The third line corresponds to our water height estimation and we can see that there is approximately a 1-mm difference with the ground truth for a change of 0.005 of the refractive index. On the other hand, these results also show that a 1-mm change of the mean water height (out of 25 cm depth) only affects the results by 2 or 3 mm, which is quite satisfying since the average value is calculated over a dispersed set of values as the water surface is dynamic.

More importantly, this study accentuates the necessity of having a better estimation of the refractive index. Maas (2015) provides the model below for the refractive index:

$$n_W = 1.338 + 4 \times 10^{-5} (486 - \lambda + 0.003d + 50S - T)$$

with n_W the refractive index of water, λ the wavelength in nm, d the depth in m, S the salinity in % and T the temperature in °C.

Using the following values: λ = 520 nm (average according to our panchromatic sensor sensitivity), d = 0.15 m (around half of maximum depth), S = 0 % (measured) and T = 22.2 °C (measured), our estimation of the refractive index in the lab is n_W = 1.33575.

4 Conclusion

Our lab experiment provides an opportunity to study the feasibility of capturing and reconstructing the water surface by images only. Several acquisition scenarios have been implemented to provide an extensive collection of data and give us the possibility to study the impact of various parameters to understand the optimal setup for our final goal of using the technique for surveying rivers later on. While we neither obtained a full nor an accurate water surface reconstruction so

	Before refraction correction	After refraction correction
Mean	65.7 mm	0.7 mm
Median	66.1 mm	0.9 mm

Table 1: Differences with the ground truth of the topography before and after refraction correction by the estimated mean water height

	Index = 1.33	Index = 1.335	Index = 1.34
Height = 1.806 m	Mean = 2.3 mm Median = 2.5 mm	Mean = 1.4 mm Median = 1.5 mm	Mean = 0.4 mm Median = 0.6 mm
Height = 1.807 m	Mean = 2.0 mm Median = 2.1 mm	Mean = 1.0 mm Median = 1.2 mm	Mean = 0 mm Median = 0.2 mm
Height = 1.8075 m	**Mean = 1.8 mm Median = 2.0 mm**	**Mean = 0.8 mm Median = 1.0 mm**	**Mean = −0.1 mm Median = 0.0 mm**
Height = 1.808 m	Mean = 1.6 mm Median = 1.8 mm	Mean = 0.6 mm Median = 0.8 mm	Mean = −0.3 mm Median = −0.1 mm
Height = 1.809 m	Mean = 1.3 mm Median = 1.4 mm	Mean = 0.3 mm Median = 0.5 mm	Mean = −0.7 mm Median = −0.5 mm

Table 2: Assessment of the refraction correction (mean and median of differences with ground truth) with different refractive index and mean water height values

far, preliminary results have shown that it is possible to gain some information on the water surface from oblique images, starting with the mean water height. We have also gained knowledge on the strong impact of the refractive index and the importance of having a proper estimation.

The main focus of our work has been on optimising the data acquisition setup to maximise the number of tie points that can be found on the water surface. However, the accuracy of these tie points is not optimal and further work is currently underway to assess the error due to specular reflection as well as to obtain more accurate tie points. Furthermore, we are also researching whether deep learning solutions for feature description and matching on images could be suitable in our case of water surface reconstruction, as such approaches have proven to provide many more tie points of high accuracy for dry and diffusely reflecting surfaces. Thus, we focus more on the post-processing side of the problem now.

Eventually, the goal is to obtain enough surface points or surface parameters, like the mean water height, wavelengths, elevation of peaks, etc., which could be used to formulate a mathematical model of the water surface. //

References

Chandler, Jim H.; Rene Wackrow; Xin Sun; Koji Shiono; Ponnambalam Rameshwaran (2008): Measuring a dynamic and flooding river surface by close range digital photogrammetry. The International Archives of the Photogrammetry, Remote Sensing and Spatial Information Sciences, XXXVII(B7), pp. 211–216

Maas, Hans-Gerd (2015): On the accuracy potential in underwater/multimedia photogrammetry. Sensors, DOI: 10.3390/s150818140

Mandlburger, Gottfried (2016): Orientation and processing of airborne laser scanning data – Module Snellius. Technical Documentation. Technische Universität Wien, https://opals.geo.tuwien.ac.at/html/stable/ModuleSnellius.html

Morris, Nigel J.W.; Kiriakos N. Kutulakos (2011): Dynamic refraction stereo. IEEE Transactions on Pattern Analysis and Machine Intelligence, DOI: 10.1109/TPAMI.2011.24

Murase, Hiroshi (1992): Surface shape reconstruction of a nonrigid transport object using refraction and motion. IEEE Transactions on Pattern Analysis and Machine Intelligence, DOI: 10.1109/34.159906

Okamoto, Atsushi (1982): Wave influences in two-media photogrammetry. Photogrammetric Engineering and Remote Sensing, 48(9), pp. 1487–1499

Over, Jin-Si R.; Andrew C. Ritchie; Christine J. Kranenburg et al. (2021): Processing coastal imagery with Agisoft Metashape Professional Edition, version 1.6: Structure from motion workflow documentation. U.S. Geological Survey Open-File Report 2021–1039, DOI: 0.3133/ofr20211039

Rupnik, Ewelina; Josef Jansa; Norbert Pfeifer (2015): Sinusoidal wave estimation using photogrammetry and short video sequences. Sensors, DOI: 10.3390/s151229828

Schönberger, Johannes L.; Jan-Michael Frahm (2016): Structure-from-motion revisited. 2016 IEEE Conference on Computer Vision and Pattern Recognition (CVPR), DOI: 10.1109/CVPR.2016.445